Computation of Unsteady Transonic Flows by the Solution of Euler Equations

V. Venkatakrishnan* and A. Jameson†
Princeton University, Princeton, New Jersey

Transonic flow over an airfoil in motion has been computed by solving the Euler equations using two methods. The finite volume scheme is used to spatially discretize the integral form of the Euler equations for a moving domain. The first method uses dissipative terms constructed according to the theory of total variation diminishing (or TVD) schemes. The TVD scheme is presented in a semidiscrete form for a scalar conservation law and then is formally extended to a system of conservation laws. The resulting system of ordinary differential equations is integrated in time by a multistage scheme. A new class of multistage schemes that preserve the TVD property is used. The technique of residual averaging, which permits the use of larger time steps, is extended to unsteady problems in a form that preserves time accuracy. The second method utilizes dissipative terms constructed from second and fourth differences in the dependent variables. Nonreflecting boundary conditions are used in the far field, allowing the use of a moving mesh.

I. Introduction

THE problem of unsteady transonic flows about moving airfoils has received considerable attention in the last decade and is of interest in flutter calculations. Many of the numerical schemes for solving unsteady problems are based on the transonic small disturbance potential equation, which is either linearized with respect to a steady flow or is solved directly, e.g., Ballhaus and Goorjian.[1] Shankar et al.[2] have solved the unsteady form of the full potential equation by an implicit method based on approximate factorization. However, schemes based on the potential equation are somewhat limited in scope, because the assumption of ignoring entropy changes and vorticity production across the shock is not strictly correct.

To describe inviscid transonic flow correctly, the Euler equations must be solved. The numerical solution of the Euler equations should provide an accurate prediction of the location of the strength of the shock and the associated wave drag. This is particularly important in unsteady transonic flow, where the small amplitude motions of the airfoil cause the shocks present in the flow to move appreciably. A number of researchers have addressed the problem of steady-state solution to the Euler equations for flows past aerodynamic configurations. In particular, Jameson and Baker[3] have solved the Euler equations for steady flow past a transonic wing-body-tail configuration, by augmenting a central difference scheme with a carefully blended mixture of second and fourth differences in the dependent variables, which acts as a dissipative term. The solution of Euler equations for flows past moving airfoils involves, in addition to accounting for time accuracy and a moving mesh, having to resolve moving shocks for which reason a numerical method with the least amount of artificial dissipation is desirable.

The Euler equations have been solved for unsteady flows by Magnus and Yoshihara,[4] Lerat and Sides,[5] Sides,[6] Steger,[8] and Chyu, Davis, and Chang.[9] Magnus and Yoshihara[4] used a finite difference scheme at the Lax-Wendroff type. Lerat and Sides[5] solved the Euler equations in integral form using the finite volume method of MacCormack with dissipative terms of the Lax-Wendroff type. Sides[6] used the implicit method of Lerat, Sides, and Daru[7] to compute unsteady flows past moving airfoils. Steger[8] and Chyu et al.[9] used implicit finite difference algorithms. There is, however, considerable scope for improvement in the solution of Euler equations for flows past moving airfoils, especially in the areas of computational speed, artificial dissipation, and the treatment of the boundary conditions.

In this paper, the Euler equations are solved for the problem of transonic flow over a moving airfoil. The finite volume scheme of Jameson, Schmidt, and Turket[10] is used to discretize spatially the integral form of governing equations for a moving domain. The resulting system of ordinary differential equations is augmented by dissipative terms constructed to obey the total variation diminishing property. These dissipative terms are derived by a formal extension of a semidiscrete TVD scheme for a scalar conservation law to a system of equations. Time marching is done by using a multistage scheme. In its original formulation,[3] this class of schemes does not necessarily preserve the total variation diminishing property. For this reason, a new class of multistage schemes, which preserve the TVD property, developed by Venkatakrishnan,[11] is used. The technique of residual averaging is also extended to unsteady problems in a form that preserves time accuracy. This technique has been found to be extremely effective in reducing the computational time. Starting from the one-dimensional work of Hedstrom,[12] non-reflecting boundary conditions have been generalized to the two-dimensional case in the far-field, allowing also the use of a moving mesh. The Euler equations have also been solved for unsteady applications by using the finite volume scheme, augmented by dissipative terms constructed by blending second and fourth differences in the dependent variables. The solutions obtained by the two schemes are compared with experimental data[13,14] as also with other computations.[5] The pressure profiles and aerodynamic coefficients very well, considering that viscous effects have been ignored altogether. Substantial improvement can be realized if one incorporates viscous effects, e.g. Ref. 8.

Presented as Paper 85-1514 at the AIAA 7th Computational Fluid Dynamics Conference, Cincinnati, OH, July 15-17, 1985; received Nov. 25, 1986; revision received Dec. 9, 1987.

*Graduate Student; currently Research Scientist, AS&M, Inc., Hampton, VA. Member AIAA.

†Professor. Member AIAA.

II. Governing Equations and Spatial Discretization

The unsteady flows of an inviscid fluid in a moving domain Ω with boundary $\partial\Omega$ are described by the Euler equations in integral form,

$$\frac{\partial}{\partial t}\iint_{\Omega} W\,dx dy + \int_{\partial\Omega} f\,dy - g\,dx = 0 \tag{1}$$

where

$$W = \begin{bmatrix} \rho \\ \rho u \\ \rho v \\ \rho e \end{bmatrix}, \quad f = \begin{bmatrix} \rho(u - x_\tau) \\ \rho u(u - x_\tau) + p \\ \rho v(u - x_\tau) \\ \rho e(u - x_\tau) + pu \end{bmatrix}$$

$$g = \begin{bmatrix} \rho(v - y_\tau) \\ \rho u(v - y_\tau) \\ \rho v(v - y_\tau) + p \\ \rho e(v - y_\tau) + pv \end{bmatrix}$$

Here p, ρ, u, v and e are the pressure, density, the Cartesian velocity components, and specific total energy, respectively. x_τ and y_τ are the Cartesian velocity components of the moving boundary $\partial\Omega$. A fifth equation is obtained from the equation of state for a perfect gas

$$e = [p/(\gamma - 1)]\,\rho + (1/2)(u^2 + v^2)$$

Assuming that the independent variables are known at the center of each cell, a system of ordinary differential equation is obtained by applying Eq. (1) separately to each cell,

$$\frac{d}{dt}(S_{i,j}W_{i,j}) + Q_{i,j} = 0 \tag{2}$$

where $S_{i,j}$ is the cell area and $Q_{i,j}$ is the approximation to the boundary integral in Eq. (1). $Q_{i,j}$ is evaluated as

$$\sum_{k=1}^{4} \Delta y_k f_k - \Delta x_k g_k$$

where f_k and g_k denote the values of the flux vectors f and g on the kth edge, Δx_k and Δy_k are the increments of x and y along the edge with appropriate signs, and the sum is over the four sides of the quadrilateral cell. The flux vectors are taken to be the averages of the values in the cells on either side of the edge and the mesh velocities as the average of the velocities of the points connected by the edge. Dissipative terms need to be added to prevent the tendency for spurious odd and even point oscillations, and to prevent overshoots or undershoots near the shock waves. Upon the addition of dissipative terms, Eq. (2) becomes

$$\frac{d}{dt}(S_{i,j}W_{i,j}) + Q_{i,j} - D_{i,j} = 0 \tag{3}$$

$D_{i,j}$ is constructed such that it is of third order in smooth regions of flow.

Two ways of constructing the dissipative term are presented. The first technique is called adaptive dissipation. Here $D_{i,j}$ is constructed from the fourth differences of the dependent variables. To capture the shock waves without substantial oscillations, an additional dissipative term is formed from the second differences of the dependent variables, with a coefficient proportional to the second difference of the pressure,

$$D_{i,j} = \left| \frac{p_{i+1,j} - 2p_{i,j} + p_{i-1,j}}{p_{i+1,j} + 2p_{i,j} + p_{i,j}} \right|$$

This coefficient is an effective sensor of the presence of a shock, and is of second order in smooth regions of flow, so that the dissipative terms are still of third order. For more details on the construction of the dissipative terms, see Ref. 15. The second method of constructing the dissipative terms utilizes the theory of TVD schemes, which is detailed in the next section.

III. Semidiscrete Total Variation Diminishing Schemes

The scheme is derived for a scalar conservation law and is then formally extended to a system of equations. For the scalar conservation law

$$\frac{\partial u}{\partial t} + \frac{\partial}{\partial x} f(u) = 0 \tag{4}$$

it is well known that the total variation

$$TV = \int_{-\infty}^{\infty} \left| \frac{\partial u}{\partial x} \right| dx$$

can never increase. Correspondingly, it seems desirable that he discrete total variation

$$TV = \sum_{i=-\infty}^{\infty} \left| u_{i+1} - u_i \right|$$

of a solution of a different approximation to Eq. (4) should not increase. Stemming from the mathematical theory of scalar conservation laws,[16] Harten[17] proposed a class of schemes that prevent the growth of the total variation of the solution, and thus eliminate the possibility of spurious oscillations. Jameson[15] has constructed a semidiscrete scheme that is similar in approach to that of Harten, and this is presented below. The advantage of the semidiscrete scheme is that one can march in time using a multistage scheme with appropriate coefficients, or by any other method.

It can be shown that a semidiscretization will have the TVD property if it can be cast in the form

$$\frac{du_i}{dt} = c^+_{i+1/2}(u_{i+1} - u_i) - c^-_{i-1/2}(u_i - u_{i-1}) \tag{5}$$

where the coefficients $c^+_{i+1/2}$ and $c^-_{i-1/2}$ are non-negative. A semidiscrete approximation to Eq. (4) is of the form

$$\frac{du_i}{dt} + \frac{1}{\Delta x}(h_{i+1/2} - h_{i-1/2}) = 0 \tag{6}$$

Denoting $f(u_i)$ by f_i, define the numerical flux in Eq. (6) as

$$h_{i+1/2} = (1/2)(f_{i+1} + f_i) - \alpha_{i+1/2}(u_{i+1} - u_i) \tag{7}$$

and suppose that

$$\alpha_{i+1/2} = (1/2)k\,|a_{i+1/2}| \tag{8}$$

where

$$a_{i+1/2} = \begin{cases} \dfrac{f_{i+1} - f_i}{u_{i+1} - u_i} & \text{if } u_{i+1} \neq u_i \\ \left.\dfrac{\partial f}{\partial u}\right|_{u = u_i} & \text{if } u_{i+1} = u_i \end{cases} \tag{9}$$

Then it follows that

$$h_{i+1/2} = f_i - (1/2)\,(k\,|a_{i+1/2}| - a_{i+1/2})\,(u_{i+1} - u_i)$$

and

$$h_{i-1/2} = f_i - (1/2)\,(k\,|a_{i-1/2}| + a_{i-1/2})\,(u_i - u_{i-1})$$

It can be verified that $c^+_{i+1/2} \geq 0$, $c^-_{i-1/2} \geq 0$ provided that $k \geq 1$. The above scheme is only first-order accurate in space.

A second-order accurate TVD scheme can be derived by applying the sequence of operations defined by Eqs. (6-9) to a corrected flux

$$F_i = f_i + g_i$$

in which g_i is an antidiffusive flux which approximates

$$\Delta x\,\alpha\frac{\partial u}{\partial x}$$

and thus cancels the first-order error. It is necessary to limit g_i, however, to prevent the possibility of $(g_{i+1}-g_i)/(u_{i+1}-u_i)$ becoming unbounded. An equivalent reasoning is that canceling all of the first-order error will result in a globally second-order accurate scheme, which has associated with it spurious oscillations. For this purpose define

$$g_{i+1/2} = \alpha_{i+1/2}\,(u_{i+1} - u_i) \tag{10}$$

and

$$g_i = B(g_{i+1/2},\, g_{i-1/2}) \tag{11}$$

where B is an averaging function, which limits the magnitude attainable by $(g_{i+1}-g_i)/(u_{i+1}-u_i)$, and satisfies the conditions

$$B(r,s) = B(s,r) \text{ and } B(r,r) = r$$

The numerical flux is now

$$h_{i+1/2} = (1/2)\,(f_{i+1} + f_i) + d_{i+1/2} \tag{12}$$

where

$$d_{i+1/2} = (1/2)\,(g_{i+1} + g_i) - \alpha_{i+1/2}(u_{i+1} - u_i) - (1/2)k\,|g_{i+1} - g_i|\,\text{sign}(u_{i+1} - u_i) \tag{13}$$

$d_{i+1/2}$ is now a controlled dissipative flux.

The averaging functions can be constructed as follows: Let r_i be the ratio of successive gradients

$$r_i = [(g_{i-1/2})/(g_{i+1/2})]$$

and set $g_i = B(g_{i+1/2}, g_{i-1/2}) = \phi(r_i)\,g_{i+1/2}$. Now the function ϕ satisfies the symmetry condition

$$\phi(r) = r\phi(1/r) \tag{14a}$$

and the consistency condition

$$\phi(1) = 1 \tag{14b}$$

A variety of functions ϕ can be considered satisfying (14a) and (14b).

$$\phi,(r) = \begin{cases} 0, & r \leq 0 \\ r, & 0 \leq r \leq 1 \\ 1, & r \geq 1 \end{cases}$$

This corresponds to defining B as the min-mod function.

Another function is due to Van Leer[18]

$$\phi_2(r) = [(r + |r|)/(1 + r)]$$

This corresponds to defining B as the harmonic mean.

$$\phi_3 = \begin{cases} 0 & r \leq 0 \\ 2r & r \leq (1/3) \\ (1/2)r + (1/2) & (1/3) \leq r \leq 3 \\ 2 & r \geq 3 \end{cases}$$

For more details on limiters, see Sweby.[19]

There are difficulties in extending the TVD scheme derived for a scalar conservation law to a system of equations, and also to equations in more than one space dimensions. First, the total variation of the solution of a system of hyperbolic equations may increase. Second, it has been shown by Goodman and Leveque[20] that a TVD scheme in two space dimensions is no better than first-order accurate. Nevertheless, dissipative fluxes can be constructed for a system of conservation laws, such that the scheme is TVD for the "locally frozen" constant coefficient system. The TVD scheme is then applied in a scalar form to each characteristic field. For this purpose, following Roe,[21] one can introduce a matrix $C_{i+1/2,j}$ with the property that

$$C_{i+1/2,j}(W_{i+1,j} - W_{i,j}) = \Delta y\,(f_{i+1,j} - f_{i,j}) - \Delta x\,(g_{i+1,j} - g_{i,j})$$

Thus $C_{i+1/2,j}$ corresponds to the mean value Jacobian matrix

$$\Delta y\frac{\partial g}{\partial W} - \Delta x\frac{\partial f}{\partial W}$$

Then $C_{i+1/2,j}$ can be diagonalized as

$$C_{i+1/2,j} = T\Lambda T^{-1}$$

where T is the matrix containing the eigenvectors of C as its columns and Λ is the diagonal matrix containing the eigenvalues of C, which are

$$\lambda_1,\, \lambda_2 = \Delta y(v - y_\tau) - \Delta x(u - x_\tau) \tag{15a}$$

$$\lambda_3,\, \lambda_4 = \lambda_1 \pm c\sqrt{\Delta x^2 + \Delta y^2} \tag{15b}$$

where c is the speed of sound. The dissipative fluxes can now be constructed according to Eq. (13) by substituting each component of $T^{-1}\,(W_{i+1,j} - W_{i,j})$ in turn for $(u_{i+1}-u_i)$. The flux limiters are similarly defined in terms of the ratios of these components between neighboring edges, while the dissipative coefficient $\alpha_{i+1/2}$ should be made proportional to the corresponding eigenvalue. The dissipative fluxes are recombined to form dissipative fluxes in the original variables $d_{i+1/2,j}$ by premultiplying it with the matrix T. This procedure is carried out in the j direction as well to yield $d_{i,j+1/2}$. The dissipative term $D_{i,j}$ in Eq. (3) is then obtained as

$$D_{i,j} = d_{i+1/2,j} - d_{i-1/2,j} + d_{i,j+1/2} - d_{i,j-1/2}$$

Following Roe,[21] the matrix $C_{i+1/2,j}$ can be evaluated by averaging the velocity component u, v and the specific total enthalpy H as

$$u = \frac{\rho^{1/2}_{i,j}\,u_{i,j} + \rho^{1/2}_{i+1,j}\,u_{i+1,j}}{\rho^{1/2}_{i,j} + \rho^{1/2}_{i+1,j}}$$

$$v = \frac{\rho_{i,j}^{1/2} v_{i,j} + \rho_{i+1,j}^{1/2} v_{i+1,j}}{\rho_{i,j}^{1/2} + \rho_{i+1,j}^{1/2}}$$

$$H = \frac{\rho_{i,j}^{1/2} H_{i,j} + \rho_{i+1,j}^{1/2} H_{i+1,j}}{\rho_{i,j}^{1/2} + \rho_{i+1,j}^{1/2}}$$

The matrix T that diagnolizes $C_{i+1/2,j}$ has been derived by Warming et al.[22] and is again evaluated at this average state. However, for most applications the simple definition

$$C_{i+1/2,j} = \Delta y\, A_{i+1/2,j} - \Delta x\, B_{i+1/2,j} \tag{16}$$

where $A = \partial f/\partial W$, $B = \partial g/\partial W$ will suffice, especially if the shocks are not too strong. Hence, Eq. (16) has been used in the unsteady calculations and is also computationally more efficient.

IV. Time Stepping

For the unsteady airfoil problems considered, the mesh moves synchronously with the airfoil, and Eq. (3) becomes

$$\frac{dW}{dt} + R(W) = 0 \tag{17}$$

where $R(W)$ is the residual

$$R_{i,j} = (1/S_{i,j})\,(Q_{i,j} - D_{i,j}) \tag{18}$$

Time marching is done by using a k-stage scheme with two evaluations of dissipative terms.

$$\begin{aligned}
W^{(0)} &= W^n \\
W^{(1)} &= W^{(0)} - \alpha_1 \frac{\Delta t}{S}\,[Q(W^{(0)}) - D(W^{(0)})] \\
W^{(2)} &= W^{(0)} - \alpha_2 \frac{\Delta t}{S}\,[Q(W^{(1)}) - D(W^{(1)})] \\
W^{(3)} &= W^{(0)} - \alpha_3 \frac{\Delta t}{S}\,[Q(W^{(2)}) - D(W^{(1)})] \\
&\cdots \\
W^{(k)} &= W^{(0)} - \alpha_k \frac{\Delta t}{S}\,[Q(W^{(k-1)}) - D(W^{(1)})] \\
W^{n+1} &= W^{(k)}
\end{aligned} \tag{19}$$

α_k is set equal to 1 for consistency. The scheme is second-order accurate in time for both linear and nonlinear problems if $\alpha_{k-1} \equiv 1/2$. In the case where the dissipative terms are constructed from second and fourth differences in the dependent variables, a five-stage scheme with two evaluations of dissipation is used. The coefficients for this scheme are

$$\alpha_1 = 1/4 \quad \alpha_2 = 1/6 \quad \alpha_3 = 3/8 \quad \alpha_4 = 1/2$$

The scheme then has an allowable courant as of 4. These coefficients are derived by considering a model problem and requiring that the scheme have good damping properties.[15]

While the TVD scheme outlined in Sec. III possesses the TVD property in semidiscrete form, in general it will lose this property when a time discretization procedure is introduced, unless the time step is made very small. For this reason, coefficients for a multistage scheme are derived such that the TVD property is preserved. This is done by considering first-order upwind discretization in space and eliminating the various stages of the multistage scheme, resulting in a multipoint single-stage explicit scheme. By appealing to the results of Jameson and Lax,[23] who have derived conditions for a multipoint scheme to have the TVD property, one obtains a system of inequalities (nonlinear in CFL numbers) that are then solved. For details, see Ref. 11. The coefficients for a three-stage scheme with two evaluations of dissipation are

$$\alpha_1 = .24 \quad \alpha_2 = 0.5$$

allowing a maximum courant number of 1.4. Coefficients for various other schemes have also been derived in Ref. 11.

The time step allowed by the three-stage scheme is very restrictive, and the technique of residual averaging is extended to unsteady problems in order to relax this restriction. This formulation differs from the implicit smoothing of Lerat and Sides[5] both in philosophy and formulation. Residual averaging is done implicitly as

$$-\epsilon_{i+1/2}\,(\bar{R}_{i+1} - \bar{R}_i) + \bar{R}_i + \epsilon_{i-1/2}\,(\bar{R}_i - \bar{R}_{i-1}) = R_i \tag{20}$$

where R_i is the residual, and $\epsilon_{i+1/2}$ is taken as

$$\epsilon_{i+1/2} = \frac{1.5}{4}\left(\frac{\Delta t}{\Delta t^*_{i+1/2}} - 1\right), \quad \frac{\Delta t}{\Delta t^*_{i+1/2}} \le 2 \tag{21a}$$

$$\epsilon_{i+1/2} = \frac{1.5}{16}\left(\frac{\Delta t}{\Delta t^*_{i+1/2}}\right)^2, \quad \frac{\Delta t}{\Delta t^*_{i+1/2}} \ge 2 \tag{21b}$$

when Δt is the time step taken, and $\Delta t^*_{i+1/2}$ is the locally allowable time step for the three-stage unsmoothed TVD scheme. The above relations were obtained by requiring that the locus of the Fourier symbol for the smoothed scheme be contained within the stability region. At the boundaries, Eq. (20) is replaced by one-sided differences such as

$$-\epsilon_{i+1/2}\,\bar{R}_{i+1} + (1 + \epsilon_{i+1/2})\,\bar{R}_i = R_i \tag{22}$$

With the incorporation of residual averaging, the allowable courant number for a three-stage TVD scheme is 5. Similar analysis is done for the non-TVD scheme allowing a Courant number of 7.5 for a five-stage scheme.

V. Boundary Condition

For the oscillating airfoil, along the moving body surface the condition

$$V \cdot \hat{n} = V_n(\text{specified})$$

is imposed. Here V is the velocity of the fluid, $\hat{n}$ is the unit normal to the moving surface and V_n is the velocity component of the moving surface in the normal direction. The pressure is extrapolated onto the airfoil. No explicit Kutta condition is specified. In the far field, we use the nonreflecting boundary conditions based on the work of Hedstrom.[12] Hedstrom has developed the conditions for a system of hyperbolic conservation laws in one space dimension by identifying the waves that leave the boundary and requiring that the solution belong to the manifold generated by the corresponding solution curves. The extension to two dimensions is

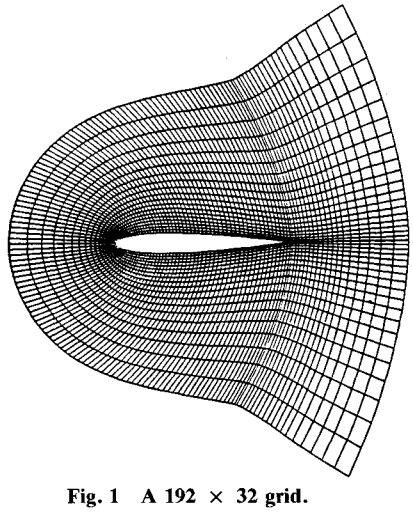

Fig. 1 A 192 × 32 grid.

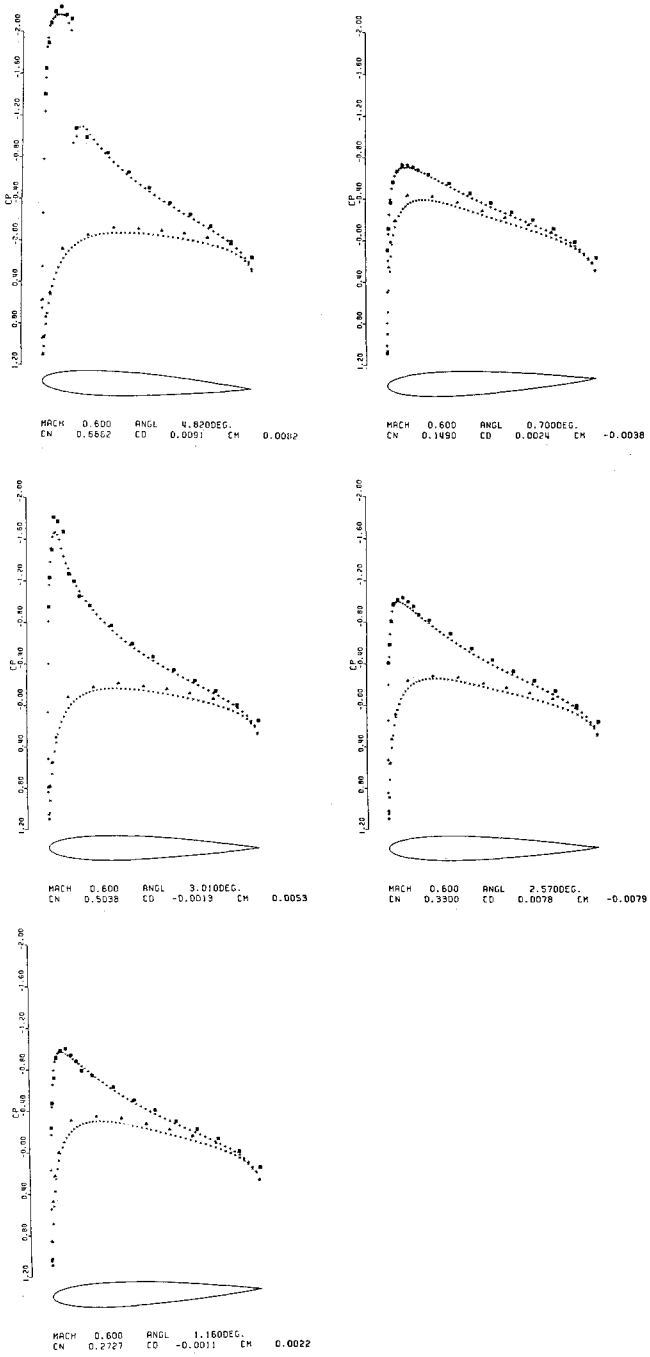

Fig. 2 Pressure profiles at various instances; AGARD CT1; computed: +, upper surface; ×, lower surface; experiment 13: ■, upper surface; ▲, lower surface.

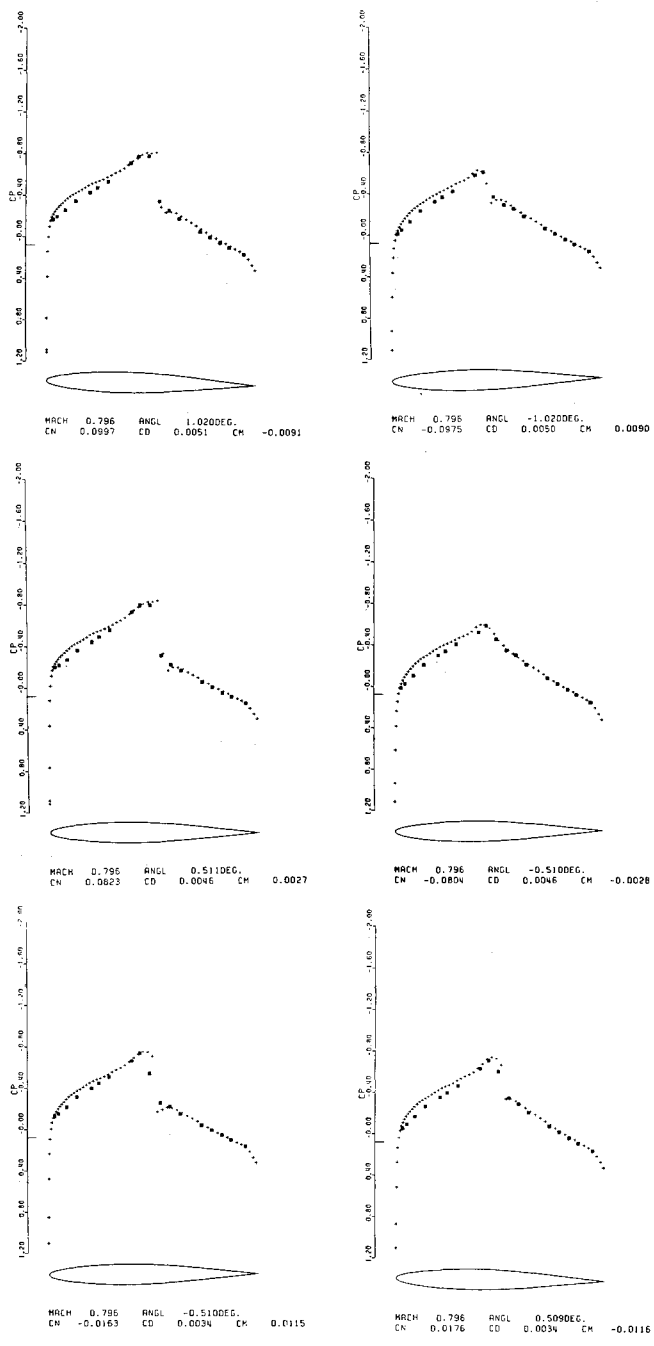

Fig. 3 Pressure profiles on the upper surface; AGARD CT6; +, computed; ■, experiment 14.

straightforward if we consider the flow locally one dimensional, and the characteristics that leave or enter the boundary are identified by the signs of the eigenvalues given by Eq. (15).

VI. Results

The airfoil computations have been performed on a 192 × 32 C grid, shown in Fig. 1. The C mesh is generated by means of a square root transformation and is then selectively stretched to compress the grid near the trailing edge. The last step is necessary, since a pressure jump at the trailing edge is observed in the unsteady calculations, and this pressure difference needs to be resolved well. The steady-state solution is obtained by running the code in the steady-state mode. This uses a five-stage scheme with two evaluations of standard dissipative terms and utilizes acceleration techniques such as local time step, enthalpy damping, implicit smoothing and multigrid strategy. The steady-state computation takes less than four minutes on the vector machine Convex C1. The airfoil is then impulsively set in motion for the unsteady calculations.

The first case computed is that of transonic flow past an oscillating airfoil, AGARD test case CT1. The motion of the oscillating airfoil is governed by the relation

$$\alpha = \alpha_m + \alpha_0 \sin \omega t \tag{23}$$

where α is the angle of attack. The frequency ω is related to the reduced frequency by the relation

$$\kappa = \omega c / 2V_\infty$$

c being the chord of the airfoil and V_∞ being the freestream velocity of the fluid. For the AGARD CT1 test case, the airfoil section is NACA0012 and the parameters are

$$M_\infty = 0.6, \quad \alpha_m = 2.89, \quad \alpha_0 = 2.01, \quad \text{and} \quad \kappa = 0.0808$$

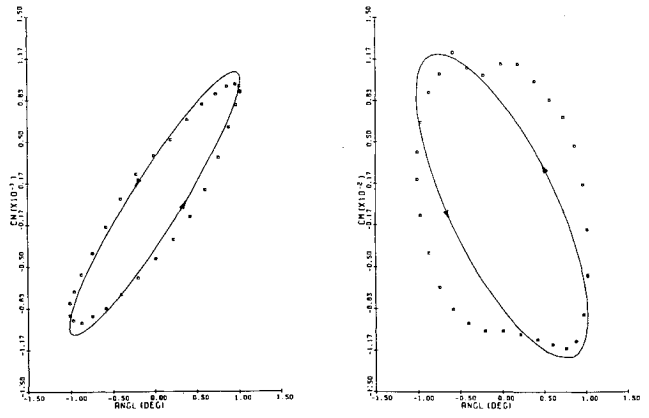

Fig. 4 Histories of lift and moment coefficients; AGARD CT6; —, computed; ■, experiment 14.

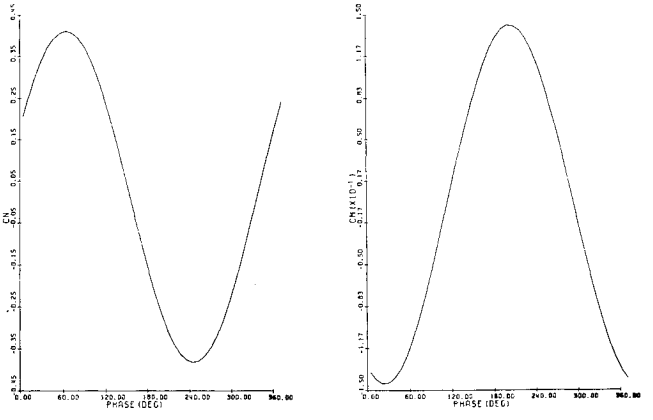

Fig. 6 Histories of lift and moment coefficients—TVD scheme.

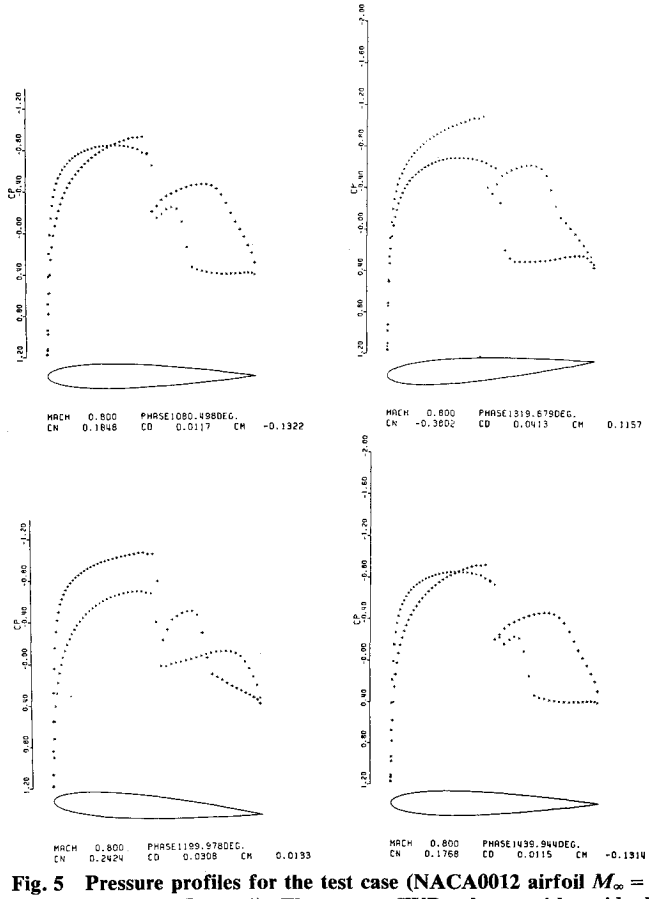

Fig. 5 Pressure profiles for the test case (NACA0012 airfoil $M_\infty = 0.8$, $\alpha_m = 0$, $\alpha_0 = 5$, $\kappa = 1$). Three-stage TVD scheme with residual averaging.

The experimental data for this case has been obtained by Landon.[13] Figure 2 shows the pressure profiles obtained using the three-stage TVD scheme and also the experimental data points at various instances during the third cycle of motion. The computed solution is nonoscillatory and the shocks, when present, are captured very well. It is clear from the pressure profiles that the shock on the upper surface moves and disappears at various stages during the cycle, and the TVD scheme, because of the limited artificial dissipation associated with it, is able to capture this phenomenon. The comparison with experimental data is excellent. The scheme used above employs a Courant number of 5. Figure 3 shows the pressure profiles on the upper surface for the AGARD CT6 test case. The airfoil section is NACA64A010 and the parameters are

$$M_\infty = .796, \quad \alpha_m = 0, \quad \alpha_0 = 1.01, \quad \text{and} \quad \kappa = 0.202$$

and experimental data has been obtained by Davis.[14] The agreement is good except for some discrepancy near the leading edge. This is due to the definition of the airfoil, since an Ames model was used in the experiment. Figure 4 shows the time histories of the lift and the moment coefficients. While the lift coefficient comparison is good, the moment comparison is unsatisfactory. In both of the test cases, the comparisons with experiments are good, taking into consideration the fact that viscous effects have been ignored altogether.

To compare the TVD scheme with the non-TVD scheme, the following case of flow over an NACA0012 airfoil has been computed:

$$M_\infty = 0.8, \quad \alpha_m = 0, \quad \alpha_0 = 5 \text{ deg}, \quad \text{and} \quad \kappa = 1$$

Figure 5 shows the results obtained using the TVD scheme, and Figure 6 shows the results obtained using the non-TVD scheme, employing second and fourth differences in the dependent variables as the dissipative term. The pressure profiles exhibit noticeable differences: the shocks are not so sharp, details are missing in the region after the shock, and the pressure peaks are consistently lower in the non-TVD scheme case. However, the aerodynamic coefficients agree very well (Figs. 7 and 8). The non-TVD scheme allows a courant number of 7.5 and takes seven minutes on the vector machine Convex C1 to compute one physical cycle. The TVD scheme uses a Courant number of 5, and takes 12 minutes on the C1 to compute one physical oscillation of the airfoil.

The final application concerns the unsteady flow over a NACA0012 airfoil oscillating in translation with great amplitude along the x-axis, at a low reduced frequency. Such a motion in the transonic regime induces important displacements of shock waves and simulates flow over a section of a helicopter rotor blade near the tip of the blade. This has been computed by Lerat and Sides using a finite volume scheme with dissipative terms of the Lax Wendroff type,[5] and also by Lerat et al.[7] by an implicit scheme. The freestream Mach number is $M_\infty = 0.536$, the angle of attack is $\alpha = 0$ and the freestream Mach number relative to the airfoil varies according to the law

$$M_{r,\infty} = M_\infty + M_0 \sin \omega t$$

where $M_0 = 0.327$ and $\kappa = \omega c/2V_\infty = 0.0925$. Solution for this problem is obtained using the TVD scheme. Figure 9 shows the unsteady pressure coefficient on the airfoil defined with respect to the freestream velocity relative to the airfoil, i.e.,

$$C_{\text{pr}} = \frac{p - p_\infty}{(1/2)\gamma\, p_\infty (M_{r,\infty})^2}$$

Only the first half-cycle of the periodic motion is presented in the figure. During this half cycle, the relative Mach number goes up from 0.536 to 0.863 and then down again to 0.536. In the second half-cycle the flow remains subsonic throughout.

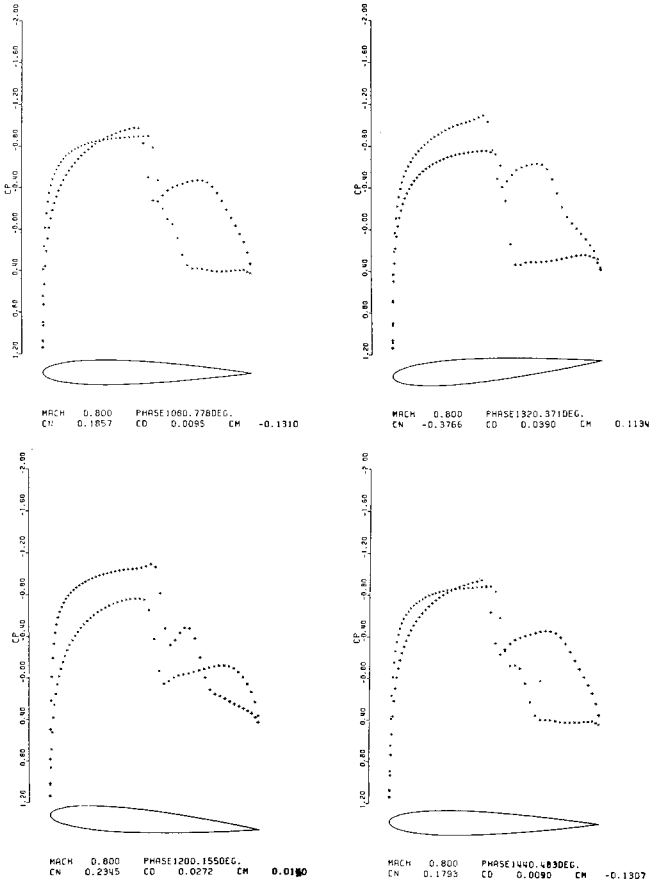

Fig. 7 Pressure profiles for the test case (NACA0012 airfoil $M_\infty = 0.8$, $\alpha_m = 0$, $\alpha_0 = 5$, $\kappa = 1$). Five-stage non-TVD scheme with residual averaging.

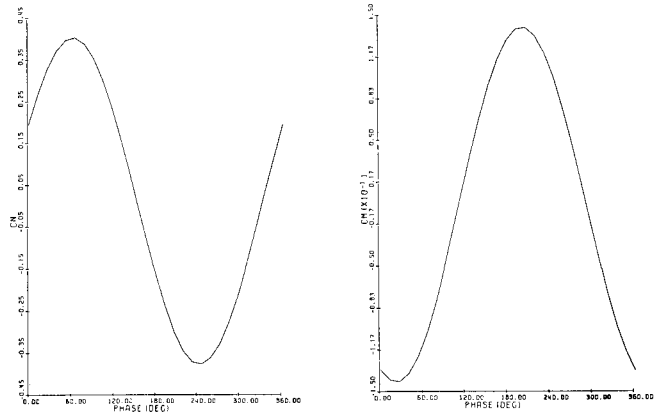

Fig. 8 Histories of lift and moment coefficients—non-TVD scheme.

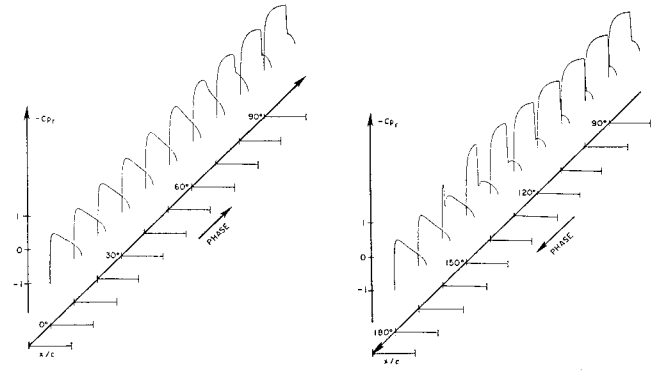

Fig. 9 Unsteady pressure distribution on the airfoil oscillating in translation.

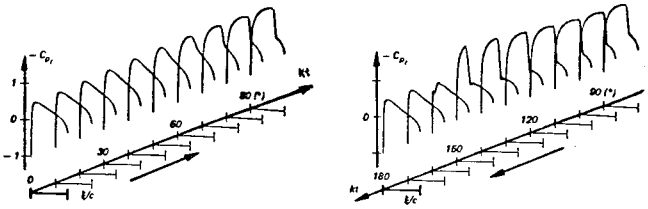

Fig. 10 Unsteady pressure distribution on the airfoil oscillating in translation—Lerat and Sides.[5]

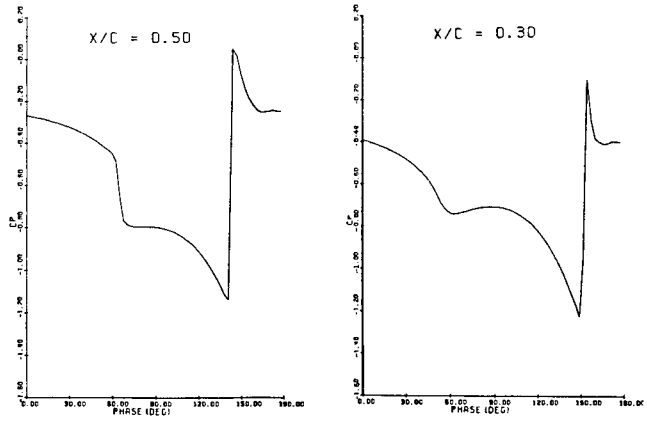

Fig. 11 Pressure traces at two points on the airfoil oscillating in translation.

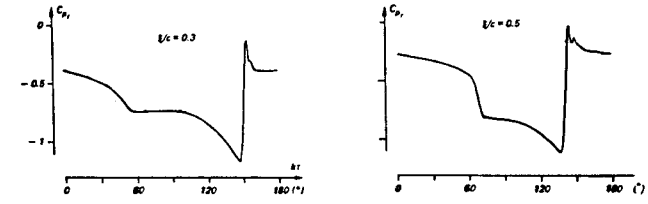

Fig. 12 Pressure traces at two points on the airfoil oscillating in translation—Lerat and Sides.[5]

From Fig. 7 we notice that a shock forms and moves downstream while gaining in strength. During the next 90 deg of the cycle, the shock wave moves upstream while weakening and then finally disappears. Figure 10 shows the results obtained by Lerat and Sides.[5] The trends are very similar. Figure 11 shows the pressure traces at two fixed points on the airfoil ($x/c = 0.3$ and $x/c = 0.5$), and Fig. 12 shows the corresponding result of Lerat and Sides.[5] There is good agreement, but the oscillations present on the pressure traces of Lerat and Sides are, as expected, absent in the present work. The above example illustrates the versatility of the present code, in that the motion of the airfoil can be arbitrary.

VII. Conclusion

The problem of transonic flow for an airfoil in motion has been addressed in this paper. The finite volume scheme is used to discretize spatially the Euler equations in integral form for a moving domain. Two ways of constructing the dissipative terms have been explored. The first method utilizes the theory of total variation diminishing schemes for constructing the dissipative terms. The TVD scheme is first presented in a semi-discrete form for a scalar conservation law and is then formally extended to a system of conservation laws. A multistage scheme, which ensures that the TVD property is preserved upon time discretization, is employed. Also incorporated is the technique of residual averaging, which allows a larger time step to be used while still maintaining time accuracy. The second method makes use of dissipative terms constructed from the second and fourth differences in the dependent variables. The problems of an airfoil pitching sinusoidally and an airfoil oscillating longitudinally are computed, and the results are

compared with experimental data and other computations. The agreement between the results obtained with the TVD scheme and the experimental data for the sinusoidally pitching airfoil is excellent. The TVD scheme is well suited for unsteady problems, providing very sharp resolutions of the shock fronts. On the other hand, the non-TVD scheme, using a blend of second and fourth differences as a dissipative term, yields reasonably accurate solutions with less expensive computations.

The finite volume formulation allows a very neat extension to the treatment of arbitrary movement and deformation of the mesh. While a rigid mesh moving with the airfoil was used in these calculations, there would be no difficulty in introducing a deformable mesh. Thus, it will be possible to treat three-dimensional flows with wing flexing or flutter analysis. The method, either with or without the TVD option, allows complete vectorization, and also distribution to multiple parallel processors. Thus, we anticipate that, with the new generation of supercomputers, three-dimensional unsteady flow simulations will be entirely feasible.

References

[1]Ballhaus, W. F. and Goorjian, P. M., "Implicit Finite Difference Computations of Unsteady Transonic Flows about Airfoils, Including the Treatment of Irregular Shock Wave Motions," *AIAA Journal,* Vol. 15, Dec. 1977, pp. 1728–1735.

[2]Shankar, V., Ide, H., Gorski, J., and Osher, S., "A Fast Time Accurate Full Potential Scheme," AIAA Paper 85–1512, *Proceedings of the AIAA 7th Computational Fluid Dynamics Conference,* Cincinnati, OH, July 1985, pp. 214–227.

[3]Jameson, A. and Baker, T. J., "Solution of the Euler Equations for Complex Configurations," AIAA Paper 83–1929, *Proceedings of the AIAA 6th Computational Fluid Dynamics Conference,* Danvers, MA, July 1983, pp. 293–302.

[4]Magnus, R. and Yoshihara, H., "Unsteady Transonic Flows over an Airfoil," *AIAA Journal*, Vol. 13, Dec. 1975, pp. 1622–1628.

[5]Lerat, A. and Sides, J., "Numerical Simulation of Unsteady Transonic Flows Using the Euler Equations in Integral Form," *Israel Journal of Technology,* Vol. 17, 1979, pp. 302–310.

[6]Sides, J., "Computation of Unsteady Transonic Flows with an Implicit Numerical Method for Solving the Euler Equations," *La Recherche Aerospatiale,* Vol. 2, No. 1985-2, March–April 1985, pp. 89–111.

[7]Lerat, A., Sides, J., and Daru, V., "An Implicit Finite-Volume Method for Solving the Euler Equations," *Lecture Notes in Physics,* Vol. 170, 1982, pp. 343–349.

[8]Steger, J. L., "Implicit Finite-Difference Simulation of Flow about Arbitrary Two-Dimensional Geometries," *AIAA Journal,* Vol. 16, July 1978, pp. 679–686.

[9]Chyu, W. J., Davis, S. S., and Chang, K. S., "Calculation of Unsteady Transonic Flow over an Airfoil," *AIAA Journal,* Vol. 19, June 1981, pp. 684–690.

[10]Jameson, A., Schmidt, W., and Turkel, E., "Numerical Solutions of the Euler Equations by Finite Volume Methods Using Runge Kutta Time Stepping Schemes," AIAA Paper 81–1259, July 1981.

[11]Venkatakrishnan, V., "Computation of Unsteady Transonic Flows over Moving Airfoils," Ph.D. Dissertation, Dept. of Mechanical and Aerospace Engineering, Princeton University, Princeton, NJ, 1986.

[12]Hedstrom, G. W., "Nonreflecting Boundary Conditions for Nonlinear Hyperbolic Systems," *Journal of Computational Physics,* Vol. 30, 1979, pp. 222–237.

[13]Landon, R. H., "NACA0012. Oscillatory and Transient Pitching," *Compendium of Unsteady Aerodynamic Measurements,* AGARD-R-702, 1982.

[14]Davis, S. S., "NACA64A010. Oscillatory Pitching," *Compendium of Unsteady Aerodynamic Measurements,* AGARD-R-702, 1982.

[15]Jameson, A., "A Non-Oscillatory Shock Capturing Scheme Using Flux Limited Dissipation," Princeton University, Princeton, NJ, Mechanical and Aerospace Engineering Rept. 1653, 1984.

[16]Lax, P. D., "Hyperbolic Systems of Conservation Laws and the Mathematical Theory of Shock Waves," *SIAM Regional Series on Applied Mathematics,* Vol. 11, 1973.

[17]Harten, A., "High Resolutions Schemes for Hyperbolic Conservation Laws," New York University Report, DOE/ER 03077-175, New York, NY, 1982.

[18]Van Leer, B., "Towards the Ultimate Conservative Difference Scheme IV. A New Approach to Numerical Convection," *Journal of Computational Physics,* Vol. 23, 1977, pp. 276–299.

[19]Sweby, P. K., "High Resolution Schemes Using Flux Limiters for Hyperbolic Conservation Laws," *SIAM Journal of Numerical Analysis,* Vol. 21, Oct. 1984, pp. 995–1011.

[20]Goodman, J. B. and Leveque, R. J., "On the Accuracy of Stable Schemes for 2-D Scalar Conservation Laws," *Mathematics of Computation*, Vol. 45, No. 171, July 1985, pp. 15–22.

[21]Roe, P. L., "Approximate Riemann Solvers, Parameter Vectors and Difference Schemes," *Journal of Computational Physics,* Vol. 43, No. 2, Oct. 1981, pp. 357–372.

[22]Warming, R. F., Beam, R. M., and Hyett, B. J., "Diagonalization and Simultaneous Symmetrization of the Gas-Dynamic Matrices," *Mathematics of Computation*, Vol. 29, No. 132, Oct. 1975, pp. 1037–1045.

[23]Jameson, A. and Lax, P. D., "Conditions for the Construction of Multi-Point Total Variation Diminishing Difference Schemes," *Applied Numerical Mathematics,* Vol. 2, No. 3–5, Oct. 1986, pp. 335–346.